Minimization of Internal Molecular Free Volume: A Mechanism for the Simultaneous Enhancement of Polymer Stiffness, Strength, and Ductility

ARTICLE *in* MACROMOLECULES · MAY 2006

Impact Factor: 5.8 · DOI: 10.1021/ma060047q

5 AUTHORS, INCLUDING:

Lokman Torun
Yildiz Technical University
26 PUBLICATIONS **327** CITATIONS
SEE PROFILE

Edwin L Thomas
Rice University
620 PUBLICATIONS **24,408** CITATIONS
SEE PROFILE

Minimization of Internal Molecular Free Volume: A Mechanism for the Simultaneous Enhancement of Polymer Stiffness, Strength, and Ductility

Nicholas T. Tsui,[‡] Alex J. Paraskos,[†] Lokman Torun,[†] Timothy M. Swager,*[,†] and Edwin L. Thomas*[,‡]

Institute for Soldier Nanotechnologies, Massachusetts Institute of Technology, 77 Massachusetts Avenue, Cambridge, Massachusetts 02139

Received January 9, 2006; Revised Manuscript Received March 2, 2006

ABSTRACT: We have synthesized and analyzed the mechanical/structural characteristics of a polyester containing 21 wt % of a triptycene monomer and compared it to a reference polyester homologue wherein benzene replaces the triptycene residue. Solvent-cast films and tension heat-treated (THT) films were investigated by tensile deformation and wide-angle X-ray scattering. The addition of triptycene units increases the T_g and, contrary to what is typically observed, also increases the ductility of film samples. In comparison to the solvent-cast non-triptycene polyester films, the triptycene polyester films displayed a nearly 3-fold increase in Young's modulus, an approximately 3-fold increase in strength, and a more than 20-fold increase in strain to failure. THT films of the triptycene polyester exhibited a modulus more than 7 times that of the non-triptycene as-cast polyester and strength greater than 14 times higher for roughly the same strain to failure. This unusually beneficial mechanical behavior is primarily attributed to the ability of individual triptycene units to express what has been termed as "internal molecular free volume" (IMFV). We suggest that the triptycene polymers adopt favorable conformations that minimize the IMFV, and the resultant assembly introduces two mechanisms for the enhancement of tensile mechanical properties: molecular threading and molecular interlocking.

Introduction

The present paradigm for producing high-performance polymers for ballistic applications is to enhance the mechanical properties by creating high axial chain alignment and strong lateral interactions between adjacent chains. Such highly aligned polymer systems exhibit great axial stiffness and strength. But since entanglements are greatly reduced in these extended chain conformations (especially in rigid-rod polymers), additional interchain interactions are necessary to transfer load between chains and to improve shear and compressive properties. While covalent bonding and hydrogen bonding have been studied in great detail as mechanisms to enhance interchain interactions, we propose that interlocking steric interactions between adjacent chains during the deformation of polymers can produce dramatic enhancements in mechanical properties. Our results serve to influence ongoing efforts to understand how to design molecular level changes to achieve high stiffness and/or high ductility and toughness. In this regard, most of the recent attention has been given to anisotropic nanoparticle additives such as carbon nanotubes[1−3] and clay sheets[4,5] which can lead to increases in stiffness and toughness while sacrificing ductility. Groups pendant to the polymer backbone have also been surveyed for their effects on the mechanical properties of polymers such as polyamides[6,7]and polyimides.[8−11] It is generally found that the attachment of rigid bulky substituents, such as adamantyl groups, while increasing T_g[12−15] actually decreases interchain interactions.[16,17] This can be understood because these pendant units interact with their surroundings essentially as spherical particles. Pendant "cage" units, such as polyhedral oligosilsesquioxane (POSS), have been examined for their ability to enhance interchain interactions due to aggregation of the POSS cages.[18−21] The behavior in those systems is dominated by the substituents around the POSS cage, and while enhancing the stiffness, the polymers suffer a decrease in ductility. Relatively little attention has been given to pendant nanoscopic rigid three-dimensional structures such as triptycenes that promote an interlocking structure between neighboring chains.

Triptycenes, as well as other fused bicyclic aromatic structures, were identified because of their unique rigid molecular geometries. One of us[22,26] introduced the notion that noncompliant structures containing triptycenes produce "internal free volume" wherein local cavities are formed because of the inability for such structures to pack efficiently (see Figure 1). This feature, which we now refer to as "internal molecular free volume" (IMFV), influences the local packing of compliant polymer chains. It has been shown that systems with these types of structures prefer to organize themselves in host materials in a way that minimizes the internal molecular free volume.[26] The triptycene molecule along with a two-dimensional representation of the qualitative process of identifying internal molecular free volume is shown in Figure 1.

The unique molecular architectures of triptycenes have attracted the interest of other researchers as interlocking elements for the creation of molecular devices such as ratchets,[23] gear systems, and propellers.[24] There has been progress toward the establishment of the molecular dynamics of such devices; however, physical products have yet to come to fruition. Recently, one of us began studies directed at exploiting the minimization of free volume to enhance the alignment of solutes in polymers and liquid crystals.[22,26] These design principles have proven robust and can dominate the organization of a system. Conventional paradigms for the organization of solutes generally rely on aspect ratio to achieve molecular alignment. It has been shown that triptycene units will exhibit orientation opposite to

[‡] Department of Materials Science and Engineering, Massachusetts Institute of Technology.
[†] Department of Chemistry, Massachusetts Institute of Technology.
* Corresponding authors. E-mail: tswager@mit.edu; elt@mit.edu.

10.1021/ma060047q CCC: $33.50
Published on Web 03/31/2006

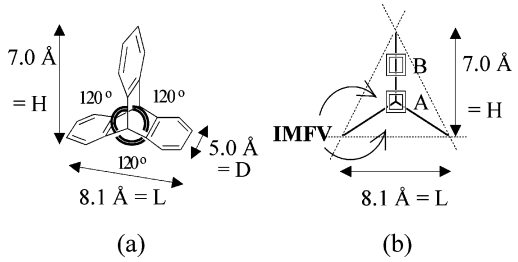

Figure 1. Triptycene molecule in (a) 3D and (b) a 2D schematic with dimensions calculated from the centroids of the hydrogen atoms at the extremities. Two types of incorporation of a triptycene unit into a polymer backbone are shown: A = bridgehead substitution and B = 1,4-benzene substitution. The internal molecular free volume (IMFV) is indicated in the two-dimensional representation as bounded by the triptycene and the dashed lines, defining an equilateral triangle of height *H* and base *L*.

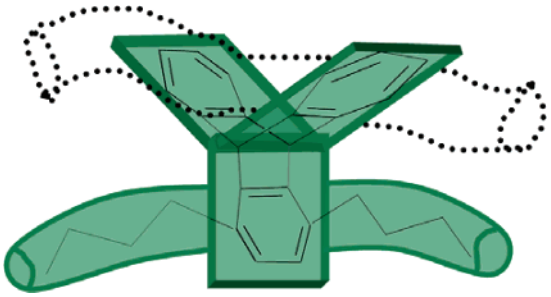

Figure 2. Triptycene unit attached to a polymer backbone (green) with a polymer chain (dotted black) threading a cavity to minimize IMFV.

what would be expected on the basis of their aspect ratio because the host molecules prefer to thread through the triptycene cavities in order to minimize the IMFV.[22]

Perhaps the earliest explorations into the effects of triptycenes in polymers was an investigation at DuPont the late 1960s wherein triptycenes were incorporated into a wide range of polymer systems.[25] In that work, triptycenes were bridgehead substituted (shown as location A in Figure 1) into the backbones of polyesters, polyamides, and polyurethanes. Solution-cast films were reported to be brittle and highly crystalline, yet clear and colorless. There was no mention of the unique geometry of the triptycene unit or its influence on the mechanical properties. Steric considerations would suggest that the attachment of the polymer chains to the bridgeheads would serve both to decrease the IMFV and to limit access to that IMFV (Figure 1). We report that triptycenes, when properly substituted, direct the organization of polymer chains via the minimization of internal molecular free volume or, specifically, the "threading" of polymer chains through triptycene cavities (shown schematically in Figure 2). The profound effects of triptycene substitution on the mechanical properties of a polyester are demonstrated.

Results and Discussion

Triptycene units were incorporated into a polyester at 21 wt % (Scheme 1) and compared to the homologous polyester without triptycene (Scheme 2). The molecular weights are displayed in Table 1. Although the molecular weight of the triptycene polyester is slightly higher than that of the non-triptycene polyester, the two polymers synthesized here have approximately equal chain contour lengths due to the additional molecular weight associated with the triptycene unit itself.

Clear and colorless films of both samples were obtained by solvent casting. Plots of storage modulus (G'), loss modulus (G''), and tan delta of these films are shown in Figure 3. The frequency dependence obeys the expected behavior. The 10 Hz

Scheme 1. Synthesis of Triptycene Polyester

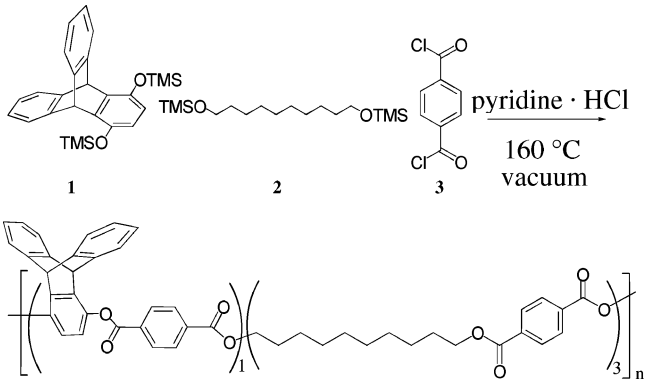

Scheme 2. Non-Triptycene Polyester

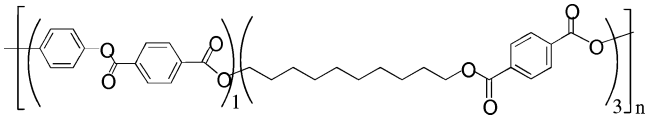

Table 1. Triptycene Polyester and Non-Triptycene Polyester M_w, M_n, and PDI Data

polymer	M_n (g/mol)	M_w (g/mol)	PDI
non-triptycene	31 900	62 000	1.94
triptycene	40 300	75 500	1.87

curve is slightly shifted such that the values for storage modulus, loss modulus, and tan delta are higher than for the 1 Hz curve. It is noticeable that the tan delta curve for the triptycene polyester is much more intense than the tan delta curve for the non-triptycene polyester, demonstrating its improved dampening properties. This difference in intensity is also indicative of the more amorphous character of the triptycene polyester as compared to the non-triptycene polyester (vide infra). The triptycene polyester displays an increased glass transition temperature from 25 to 55 °C (taken from the 1 Hz tan delta curve). DSC results show a decreased melting temperature from 119 to 93 °C and a reduced heat of melting with respect to the non-triptycene polyester, indicating that the inclusion of the bulky triptycene unit decreased crystallinity in the samples. The thermal properties from DMA and DSC are summarized in Table 2. From the storage modulus curves, it can be seen that, at room temperature, the triptycene polyester displays a significantly higher modulus value than the non-triptycene polyester. The addition of triptycene extends the glassy plateau well past room temperature, while the non-triptycene polymer has its glass transition around room temperature. However, dynamic mechanical analysis (DMA) indicates that when both polymers are in their glassy regimes, their modulus values are comparable.

Tensile tests conducted on the solvent-cast films showed sample moduli in agreement with the observations from the DMA. Comparative tensile stress−strain curves are shown in Figure 4, and the tensile mechanical properties data are summarized in Table 3. While the difference in modulus between the two samples at room temperature may be mostly attributed to the shift in glass transition temperature, the triptycene polyester also displayed significantly higher strength and higher strain to failure. The latter behavior was an unexpected result, since the triptycene polyester is still in its glassy plateau at room temperature. Additionally, the non-triptycene polyester, despite being beyond its glassy plateau, displayed low ductility as compared to the triptycene polyester. To ensure that this was not due to some sort of solid-to-

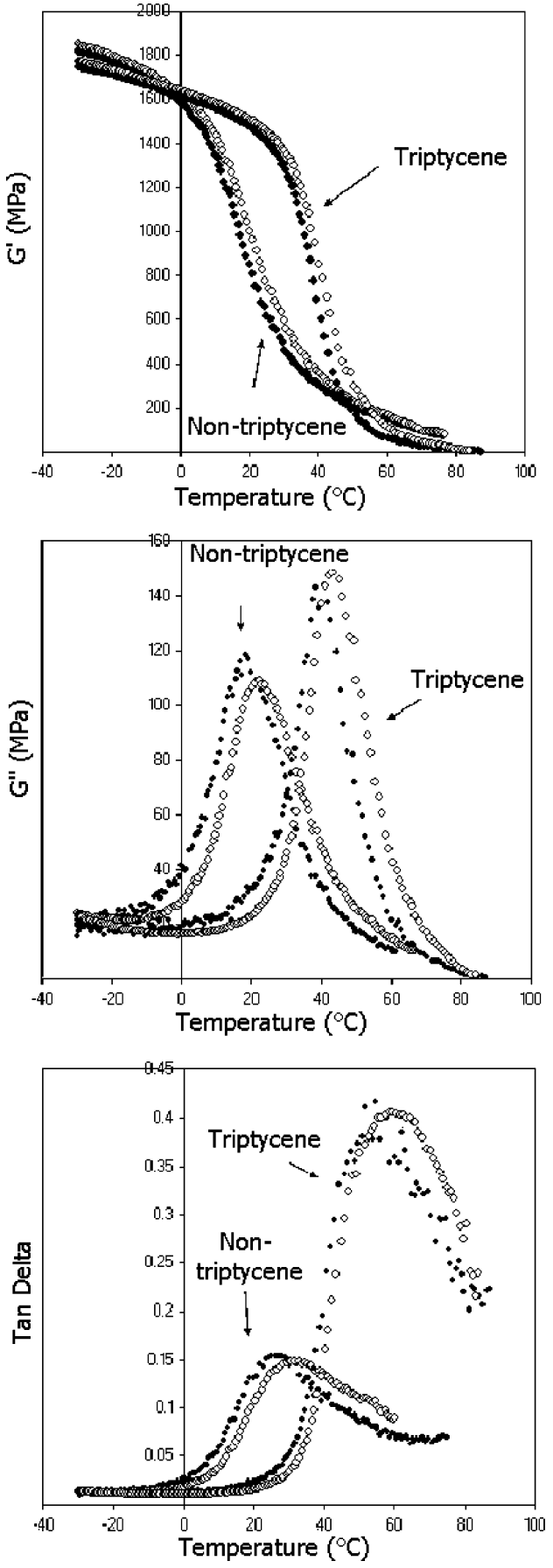

Figure 3. DMA of triptycene containing polyester vs non-triptycene polyester. The open circles indicate a frequency of 10 Hz, and the closed circles indicate a frequency of 1 Hz.

Table 2. Summary of the Polymer's Thermal Properties

polymer	T_g (°C)	T_m (°C)	ΔH_m (J/g)	$T_{d,air}$ (°C)
non-triptycene	25	119	27.9	375
triptycene	55	93	11.8	382

viscoelastic fluid transition around T_g, tensile tests were also conducted at −30 °C, a temperature well below the T_g's of both polymers.

At −30 °C, the modulus of the non-triptycene polyester increased in accordance with the DMA results, and the ductility dropped sharply (from 10% at room temperature to ∼1.4% at −30 °C) as would typically be expected for a polymer transitioning into its glassy regime (see Figure 5). The sub-T_g environment's failure to enhance the ductility confirmed that the non-triptycene polyester's lack of ductility at room temperature had nothing to do with a transition to a viscoelastic fluid because of the proximity to its T_g. As expected, the triptycene sample maintained a similar modulus (the mean of 1.58 GPa at −30 °C was slightly lower than the room temperature mean of 1.62 GPa, but this is attributed wholly to statistical variation as 0.04 GPa is well within one standard deviation of either measurement) while producing higher strengths at the point of neck formation. This increase in strength was due to the yield point (neck formation) occurring at a higher strain at −30 °C ($\epsilon \sim 6\%$) than at room temperature ($\epsilon \sim 2-3\%$), a side effect from the reduced molecular motions at lower temperatures. The triptycene samples failed prematurely in the grips before necking had reached both ends of the sample. Therefore, no work hardening was seen because of the increased defect sensitivity at the lower temperatures.

Both of the as-cast polyester films were optically clear; however, the tension heat-treated (THT) triptycene polyester films had varying levels of opacity down the length of the film (non-triptycene polyester films could not be tension heat-treated; see Experimental Section). This was probably due to sample necking. During the THT process, the parts of the film that first undergo necking contain chains in more extended conformations at the elevated temperature for longer periods of time than other parts of the film due to the neck propagation. This resulted in the variation of crystallinity along the length of the stretched film (> 25 cm long), which caused the varying levels of opacity in individual film samples tested (4 cm gauge length samples). Tensile tests of the THT films at room temperature yielded

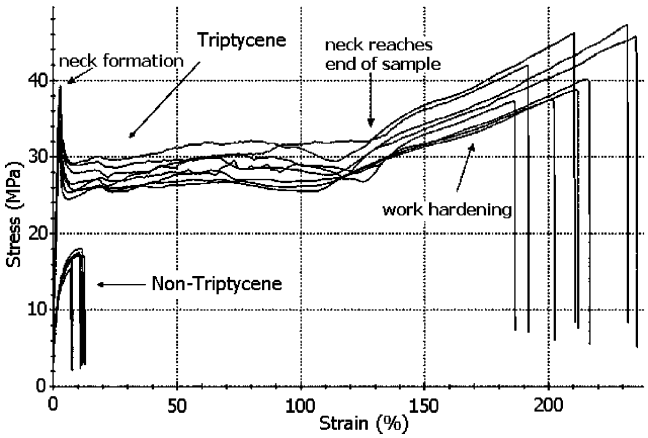

Figure 4. Tensile properties of triptycene and non-triptycene polyester films at room temperature. The presence of triptycene resulted in average percent increases of 180% for modulus (1.62 GPa compared to 0.58 GPa), 150% for strength (42 MPa compared to 17 MPa), and over 2000% for strain to failure (211% compared to 10%). The "highest individual result" samples for the triptycene polyester are not shown to prevent clutter.

Table 3. Summary of Film Tensile Tests for the Polymers

polymer film	t (μm)[b]	ρ (g/cm^3)[b]	E (GPa)[b]	σ (MPa)[b]	ϵ_b (%)[b]	work (J/cm^3)[b]
non-triptycene	80 ± 3	1.20 ± 0.01	0.58 ± 0.03	17 ± 1	10 ± 2	1.50 ± 0.25
		HIR:[a]	0.70	23	11	2.50
triptycene	87 ± 13	1.18 ± 0.01	1.62 ± 0.11	42 ± 4	211 ± 17	66.25 ± 8.25
		HIR:[a]	1.95	62	224	83.75
triptycene THT[a]	38 ± 8	1.21 ± 0.01	4.63 ± 0.36	274 ± 27	11 ± 2	18.50 ± 3.25
		HIR:[a]	5.10	326	12	22.50

[a] THT = tension heat treated film samples. HIR = highest individual result. [b] t = thickness, ρ = density, value given in parentheses is for one standard deviation.

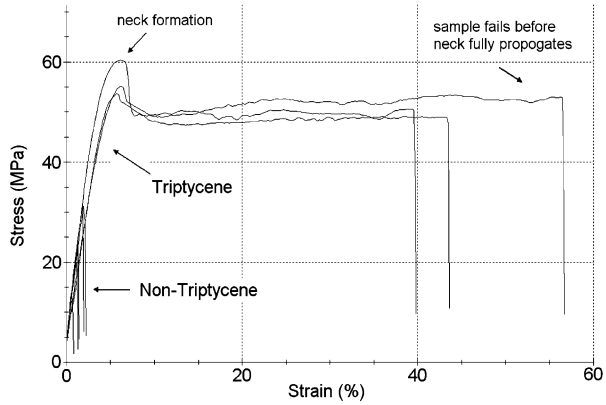

Figure 5. The −30 °C tensile properties of non-triptycene films yield a modulus (E) of 1.61 ± 0.10 GPa, strength (σ) of 24 ± 8 MPa, and strain to failure (ϵ_b) of 1.4 ± 0.5%, while triptycene polyester films exhibit a modulus (E) of 1.58 ± 0.13 GPa, strength (σ) of 55 ± 6 MPa, and strain to failure (ϵ_b) of 47 ± 9%.

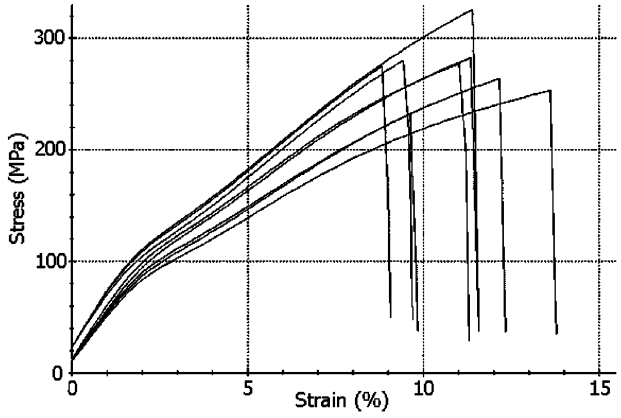

Figure 6. Room temperature tensile properties of THT triptycene polyester films.

average values of 4.63 GPa for modulus, 274 MPa for strength, and 11% for strain to failure. The results are summarized in Table 3, and the stress−strain curves are plotted in Figure 6. The highest individual THT film results exhibited a modulus of 5.10 GPa, strength of 326 MPa, and a strain to failure of 12%. As expected, this oriented film displayed a higher density than the as-cast triptycene film (Table 3).

It is interesting to note that even though the triptycene polyester films lost a great deal of ductility during the THT processing (which is expected), they still exhibited ductility comparable to if not slightly higher than the as-cast room temperature non-triptycene polyester films. When compared with the −30 °C non-triptycene films, the THT triptycene polyester films displayed on average almost 3 times the modulus, over 11 times the strength, and almost 8 times the strain to failure.

Wide-angle X-ray scattering (WAXS) shows that the addition of the triptycene units (while lowering the crystallinity) does not appear to change the type of crystal formed, since nearly

Table 4. WAXS *d*-Spacings (Å) of the Polymer Films

non-triptycene[a]	3.9	4.4	5.5		15.9
triptycene[a]	3.9	4.3	5.5		16.0
triptycene strained[b]		4.3		6.5	15.9
triptycene THT[a]		4.3		6.4	15.8

[a] The as-cast and tension heat treated samples were not deformed prior to WAXS. [b] The strained triptycene sample was elongated over 200%.

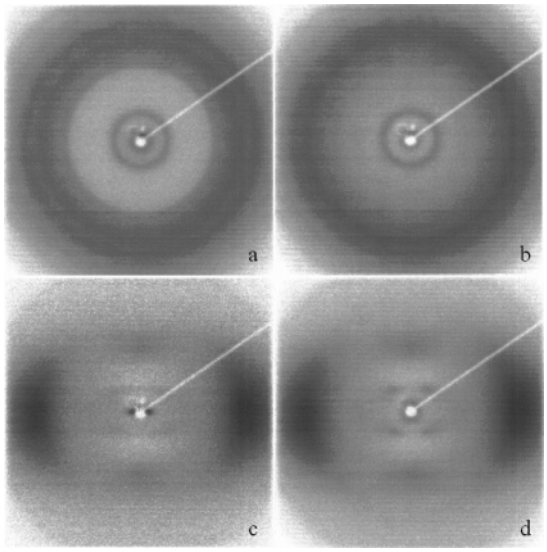

Figure 7. WAXS of (a) non-triptycene polyester as-cast film, (b) triptycene polyester as-cast film, (c) triptycene polyester strained over 200%, and (d) THT triptycene polyester. The stretching direction and THT direction are along the vertical axis.

the same *d*-spacings are present for both samples. Table 4 summarizes the observed *d*-spacings seen in Figure 7. Both types of as-cast films displayed isotropic rings as expected. Figure 7c shows an X-ray pattern taken of a triptycene polyester film after stretching over 200%. A broad pair of equatorial arcs corresponds to a peak present in the isotropic sample at about 4.3 Å, and the ring at about 16 Å breaks up into four distinct spots oriented at ∼60° from the equator. While the two peaks at 3.9 and 5.5 Å are no longer distinguishable, the breadth of the arcs is from 3.5 to 5.7 Å. Therefore, it is possible that these peaks are present in the oriented samples, but they are no longer distinguishable from the 4.3 Å peak. A pair of additional arcs also appears that is not evident in the isotropic samples. These arcs and spots indicate the anisotropy imparted during the deformation process. Figure 7d shows the WAXS of a THT triptycene polyester film. The pattern is nearly identical to that of the room temperature strained triptycene sample, but the four inner spots at about 16 Å are more intense. The full width at half-maximum of the 4.3 Å equatorial peak for both samples also confirmed that the THT process produced films with slightly higher levels of orientation as the azimuthal spread was 5° for the THT film and 6° for the room temperature strained triptycene film. WAXS *d*-spacings for all of the samples are summarized in Table 4 and were acquired by integrated circular

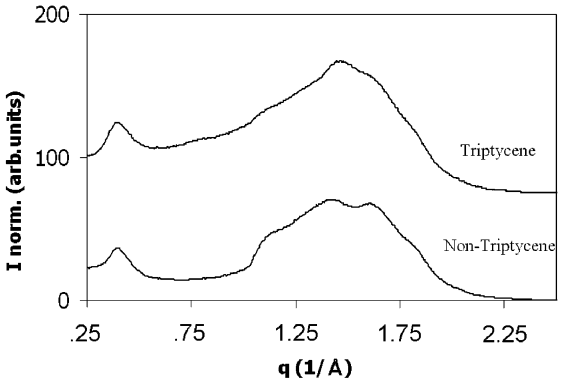

Figure 8. Integrated circularly averaged scans of the WAXS patterns in Figure 7a,b.

scans shown in Figure 8. Because of the anisotropy present in the strained and THT triptycene polyester samples, additional sector integrations were performed to probe the *d*-spacings in each direction. Three scans were taken with an azimuthal angular width of 10° about a particular direction: equatorial, meridional, and at an azimuthal angle of 60°. The sectors are shown in Figure 9, and the observed *d*-spacings are noted in Table 5.

The unique mechanical enhancements and structural properties we have observed must have their origins in the triptycene unit. We further believe that these dramatic effects are best described by the steric mechanisms induced by the system's desire to minimize its internal molecular free volume (IMFV). As was proposed in the chromophore alignment studies,[22,26] sections of polymer chains prefer to thread through the cavities of triptycene units. Figures 2 and 10 display schematically how this type of threading differs from traditional notions of threading the eye of a needle. The types of threading used here have much fewer restrictions on the polymer chain conformations needed to occupy a triptycene cavity. The mere presence of pendant rigid triptycene units along the backbone of a

Table 5. WAXS Results from Equatorial (−5° to 5°), Meridional (85° to 95°), and 60° Azimuthal Angle (55° to 65°) Scans

	d-spacings (Å)		
polymer film	equatorial	meridional	60°
triptycene strained	4.2	6.5	15.9
triptycene THT	4.2	6.5	15.9

polymer coupled with the occupation of triptycene cavities with portions of neighboring polymer chains would be expected to reduce dramatically the molecular chain mobility. In accordance, we see a large increase in the glass transition temperature of the triptycene polymer relative to the non-triptycene homologue. While the enhancement of the stiffness of the polymer with triptycene is therefore expected, the increases in strength and strain to failure are not. It can be seen from the stress−strain curves that the high strength values can be attributed to the work hardening that occurs at high strains ($\epsilon > 130\%$). We suggest that the enhanced work hardening in this case occurs due to triptycene−triptycene interactions. Typical bulky groups will slide by one another during the deformation process without large interactions because they are not directed into an interlocking structure by IMFV. However, triptycene units mutually threading along each other's chains will tend to interlock at high strains (Figure 10).

The particular strain level at which this occurs and the extent to which it increases the strength will depend on the relative amount of triptycene in the backbone. We also observe a large region of deformation (the neck propagation) before the work hardening initiates. Neither necking nor work hardening occurs in the non-triptycene polymer. We attribute this behavior to triptycene−chain interactions. In the non-triptycene polymer, the lateral chain interactions are very weak. This is why the strain to failure is so low despite the sample being above its T_g at room temperature. The polymer chains threading through the triptycene units give the triptycene polymer enhanced lateral interactions without the loss of ductility that would accompany

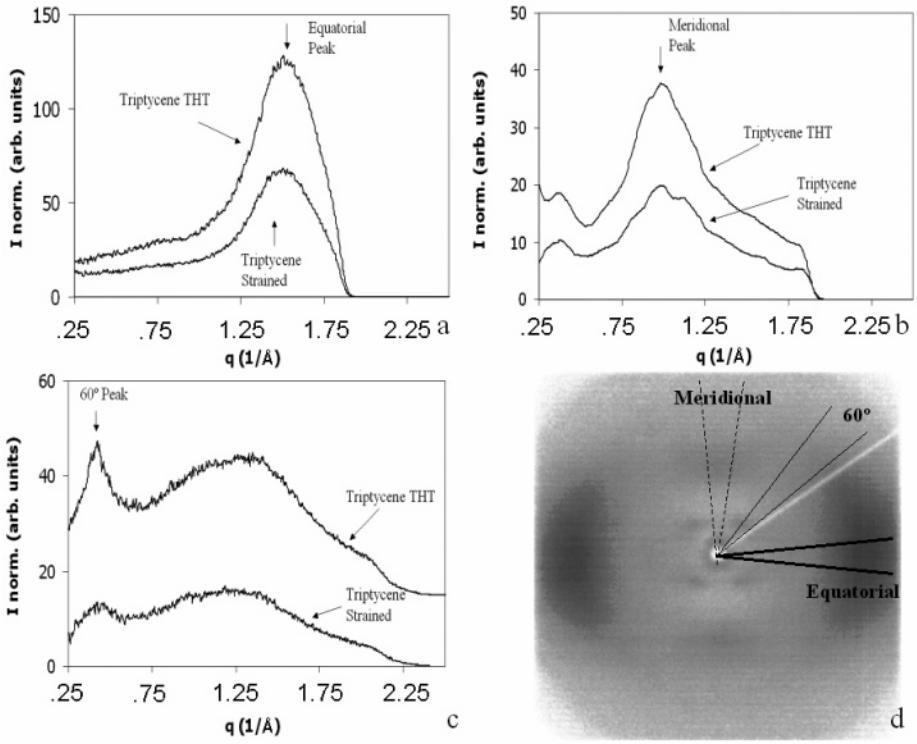

Figure 9. (a) Equatorial, (b) meridional, and (c) 60° sector scans in WAXS of strained and THT triptycene polyester films. (d) shows the angular definitions of each scan.

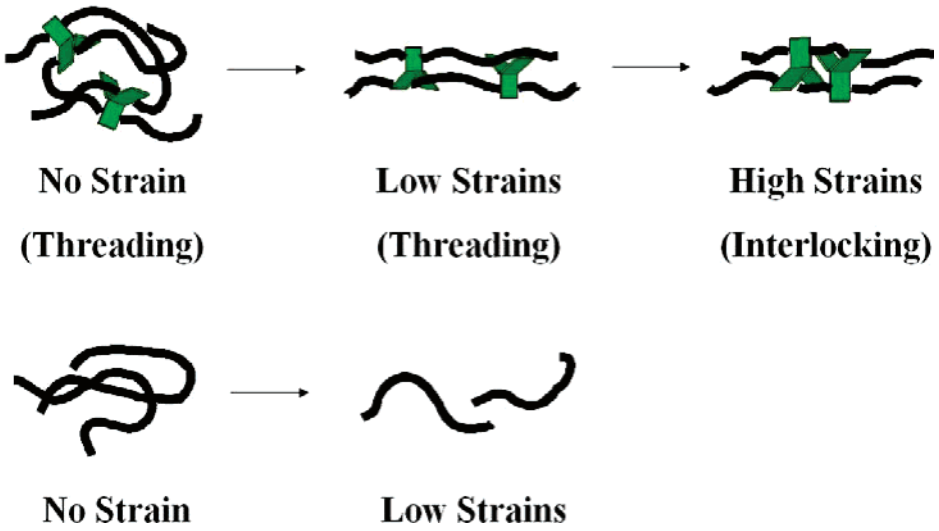

Figure 10. Schematic of the steric interactions induced by the triptycene unit and the minimization of IMFV. The same polyester without triptycene fails at low strains due to poor lateral interactions.

interchain covalent bonding. This promotes the large deformations observed. Mutual threading of triptycene units would also induce parallel alignment of the neighboring chains, further aiding in the orientation process during deformation. The triptycene units, and therefore their effects on the mechanical properties, are randomly and homogeneously distributed throughout the system, and the mechanical properties observed are an average over all chain segment motions and interactions. Thus, the influence on chain segment movement appears macroscopically as similar to enhanced chain entanglement. In the necking region, the dominant interaction was that of threading, but as the interlocking mechanism became more prominent at high strains, the work hardening regime reflected that in a new, but still constant, influence on mechanical properties. The threading of polymer chains through triptycene clefts does not generate a characteristic signal in WAXS as such a spatial correlation would be too weak to resolve in the presence of crystalline peaks. Density measurements show that the non-triptycene polyester as-cast film has a slightly higher density than the triptycene polyester as-cast film. However, the increase in density associated with the threading of polymer chains through triptycenes must compete against the decrease in density resulting from the loss in crystallinity. In the THT triptycene polyester films, the density is higher than in the non-triptycene as-cast film, as might be expected, since it is an oriented sample. While it is not rigorous proof, the comparable densities suggest that threading may indeed be occurring, since triptycenes would be expected to decrease density by much more than 0.02 g/cm^3 given the loss of crystallinity coupled with the shear bulkiness of the triptycene units in the absence of threading. Still, the most compelling evidence for molecular threading and molecular interlocking is the mechanical properties that result from the addition of triptycene.

The ability for threading and interlocking to affect the mechanical properties of a polymer depends on the percentage of the contour length of the chain that is influenced by the minimization of IMFV. As shown in Scheme 1, there are three major components to the triptycene polyester: (1) the triptycene, (2) a long aliphatic decane, and (3) a terephthaloyl connector. The long aliphatic component is the most likely candidate at equilibrium for threading through the triptycene cavities. Using a triptycene cavity width of 7.4 Å (see Figure 11) and the overall contour length of the mer of about 76 Å, about 10% of the contour length of the chain is affected by the threading of one

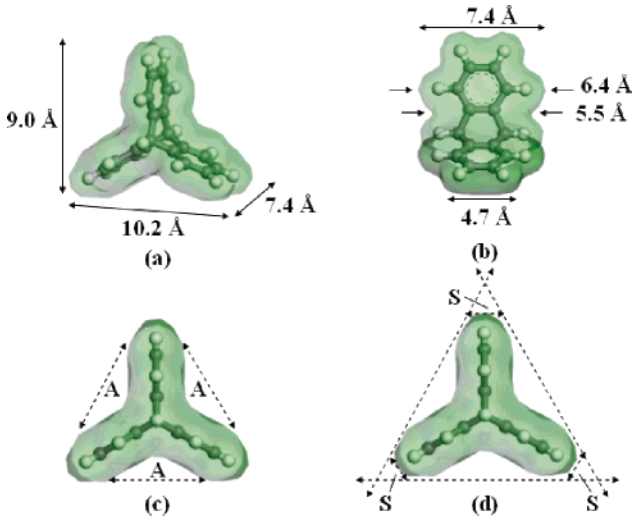

Figure 11. Space-filling (van der Waals isosurface) triptycene models showing (a) three-dimensional view, (b) width measurements along the triptycene axes, (c) method 1 where A is the cleft space, and (d) method 2 where S is the extra space outside of the triptycene unit when enclosed in a triangular prism.

triptycene cavity. Since both chains are affected by threading, in the case of two chains mutually threading one another's triptycene units (as in Figure 10), 20% of the contour length of the chain is now affected. Since the triptycene in actuality has three available cavities and three aliphatic components per mer, this model can be extended in three dimensions, allowing each mer to participate in four threading interactions. Therefore, a possible 40% of the contour length of a polymer chain can be under the influence of IMFV. During deformation, the occupation of the triptycene cavities is no longer restricted to the aliphatic components. Even though the terephthaloyl connector is a bulkier unit and thus may not reside as "deeply" inside of a triptycene cavity, it is still susceptible to the attractive force related to the minimization of IMFV.

There are many units like triptycene that also contain IMFV, but there currently exists no way to analyze a candidate structure's ability to utilize this to enhance the properties of a polymer. There is not even a method to estimate an amount of IMFV in a particular unit. The simple schematic in Figure 1 provides an elementary starting point but is inadequate in providing an estimate of the IMFV for an isolated triptycene

unit because it neglects the volume of the structure itself. Values for the IMFV of a single triptycene unit calculated in this way overestimate the actual amount of available free space in any particular structure. Thus, there is a need both qualitatively and quantitatively to define this structural property. We define IMFV as "the difference in volume between that which is generated by the geometry of the structure and that occupied by the structure itself." The volume that the structure occupies can be calculated, for example, by using Materials Studio software. There are multiple ways to calculate the volume generated by the geometry of triptycene-like structures; therefore, two different methods for the determination of IMFV are presented here. Both methods are conceptually developed in Figure 11.

The first proposed method is a direct geometric calculation of the internal cavities created by the structure. This method does not require the measurement of the volume that the structure itself occupies or the proper assignment of a volume swept out. The different spaces defined in Figure 11c represent the portions used to calculate the total IMFV. These volumes could be measured in a number of ways. One approach is to use the symmetrical cavities labeled A, which are approximated as triangles defined by the van der Waals surfaces of the phenyls. As seen from Figure 11b, the maximum width of the cavities (defined by the para-hydrogens of the phenyls) is 7.4 Å. The IMFV by this model for an individual triptycene is $3 \times A \times 7.4\ \text{Å} \approx 93\ \text{Å}^3$.

While this first method is the endorsed routine for the calculation of IMFV by the authors, in the event of any unforeseen complications due to a particular structure, we also present a second method. This method is more simplistic but can be used as a quick approximation. The general procedure is to determine the volume swept out by the geometry and then subtract off the volume occupied by the structure. To determine the volume swept out by the geometry of the structure, simply identify the smallest convex polyhedron that fully encloses the structure. A triangular prism is the most efficient polyhedron for this purpose (Figure 11d) and can furthermore be packed into a perfectly dense extended structure. This simple polyhedron will overestimate the total volume assigned to a triptycene unit because it does not properly account for the rounded shape of the isosurface near the corners. To correct for this, the small triangular prisms labeled S need to be subtracted. But perhaps more significantly, because of the varying width of the triptycene structure (Figure 11b), using the extremity of 7.4 Å as the width value will further assign spaces along the triptycene axes as internal molecular free volume. The ability of these irregular spaces to contribute to IMFV will depend on the polymer conformations, and presently, it is not possible to determine the fractional occupancy. For this reason, these spaces were neglected in method 1. Therefore, this second method overestimates the IMFV at 202 Å^3 (without the subtraction of the S spaces, the IMFV $\approx$ 218 Å^3). It can be seen that the overestimation of the IMFV of the triptycene by method 2 is almost completely dominated by the variations along the width of the triptycene. These types of variations will be specific to the particular structure of interest, and therefore, this second determination will not necessarily overestimate IMFV by the same amount from unit to unit. Because of its simplicity and intuitiveness, the authors felt that method 2 had to be acknowledged; however, for the reasons stated, we support the usage of method 1.

It is important to note that our methods for the calculation of IMFV only apply to isolated units. A complete understanding of the system would require consideration of complex synergisms between components, distributions of conformations, and allowances for the inherent chemical irregularities of a random copolymer. For example, by placing the polymer backbone at the bridgehead positions (Figure 1), the polymer chains partially block access to all three of the concave clefts defined by the triptycene structure. This will prevent unrestricted access of neighboring polymer chains to those sites of IMFV. In our triptycene polyesters, the connection of the polymer chains at only one of the phenyl rings (Figure 1) leaves one cleft completely open for occupation (threading) by a neighboring polymer chain. In addition, the fact that this connection is made through an ester group, which can lay coplanar with the phenyl ring, imposes minimal steric obstruction to the directly adjacent clefts. The accessibility of IMFV creates the need for an additional distinction. The IMFV calculated by our general method assumes full accessibility and therefore will be called "inherent" IMFV. In the case of the triptycene polyester used in this study, this would result in 40% of the contour length of the chain being influenced by the minimization of IMFV. However, in any given system, there will be an "effective" IMFV, which should take into account any limitations to the accessibilities of the inherent IMFV specific to that system. It should be also noted that it is possible for the effective IMFV to be greater than the inherent IMFV because a particular type of incorporation may enhance the spatial influence of an individual structure. For example, if a particular moiety is threading through a triptycene cleft, there will be some persistence length over which the moiety is forced into mutual alignment with the triptycene cleft. Therefore, the effective IMFV is the volume over which triptycenes and similar types of structures influence the local packing of their surroundings. It is much more difficult to quantify the effective IMFV, and that process is not detailed in this work.

Conclusions

The incorporation of triptycene units into the backbone of a polyester at 21 wt % significantly increased the modulus, strength, and strain to failure for solvent-cast films, marking the simultaneous improvement of both stiffness and ductility. This was an unusual result because it is typically observed that enhancements in stiffness lead to sacrifices in ductility. There exists no general method of achieving such simultaneous enhancements exclusively with a homopolymer. These results indicate that the steric influence of rigid, pendant units may facilitate new advances in the enhancement of the mechanical properties of polymers. The specific types of steric interactions suggested here (molecular threading and molecular interlocking) are directed by the system's desire for the minimization of internal molecular free volume about the triptycenes. These new types of interchain interactions from the incorporation of designed shape persistent structures allow access to combinations of properties that are not presently accessible from conventional systems that rely on chain−chain interactions arising from cross-linking, hydrogen bonding, ionic bonding, or crystallization to achieve high strength.

Experimental Section

Material Synthesis. The triptycene polyester was synthesized by melt polymerization with 1,4-di(trimethylsilyloxy)triptycene **(1)** 1,10-bis(trimethylsiloxy)decane **(2),** and terephthaloyl chloride **(3)** at 165 °C under vacuum in the presence of catalytic amount of pyridine hydrochloride.[27] Compounds **1**−**3** (Scheme 1) were mixed under nitrogen and heated to 165 °C. Addition of a catalytic amount of pyridine·HCl resulted in in-situ deprotection of compounds **1** and **2**, which then reacted with terephthaloyl chloride (**3**) overnight

(Scheme 1). Similarly, non-triptycene polyester (Scheme 2), in which a benzene replaces the triptycene moiety, was also prepared with 1,4-di(trimethylsiloxy)benzene as an analogous polymer for comparison.

1,4-Di(trimethylsilyloxy)triptycene (1). Triptycene-1,4-hydroquione[28] (29.3 g, 102 mmol) and imidazole (17.4 g, 256 mmol) were placed in a two-necked 2 L flask with a magnetic stir bar. The flask was purged with argon, and then 1 L of dry THF was added via a cannula. Chlorotrimethylsilane (32.5 mL, 256 mmol) was added, and the reaction was heated to reflux with stirring for 19 h, when it was cooled to room temperature and filtered. The solvents were removed in vacuo, and the remaining solid was filtered through two separate silica gel pads with CH_2Cl_2. Upon removal of the solvents, 43.1 g (100 mmol, 98%) of pure **2** remained as a white solid, which was dried under vacuum at 80 °C overnight before being used for polymerizations. ^{1}H NMR ($CDCl_3$, δ): 0.30 (s, 18H, TMSO), 5.70 (s, 2H), 6.35 (s, 2H), 6.96−6.99 (m, 4H, Ar−H), 7.36−7.39 (m, 4H, Ar−H). ^{13}C NMR (CDCl3, δ): 0.6, 48.1, 117.0, 123.7, 124.8, 136.6, 144.4, 145.6. IR (KBr, cm^{-1}): 3065, 3022, 2956, 1583, 1480, 1255, 1009. HRMSEI (*m*/*z*): (M+) calculated for $C_{26}H_{30}O_2$ 430.1779; found 430.1768.

General Procedure for Melt Polymerizations. In a drybox, 1,-10-bis(trimethylsiloxy)decane was placed in a 50 mL Schenk flask, after which the appropriate ratios of bis(trimethylsiloxy)triptycene and terephthaloyl chloride were added. The flask was sealed with a septum, brought out of the glovebox, and attached to a vacuum/gas line under an argon atmosphere. The flask was heated to 155 °C with stirring until all of the solids had melted to give a yellow liquid. Pyridine hydrochloride (20 mg) was quickly added, and the reaction was allowed to stir at 155 °C for 10 min. Another 20 mg of pyridine hydrochloride was added, and the stirring was continued for 1 h. During this time the flask was frequently vented by placing a needle through the septum while the reaction was under a positive pressure of argon. Another 100 mg of pyridine hydrochloride was added, and the reaction was stirred at 155 °C for an additional 1 h, after which it was heated to 170 °C for $^1/_2$ h. By this time the reaction was highly viscous, and only a very slow stir rate was possible with a magnetic stirrer. The reaction was heated to 180 °C and placed under vacuum overnight with slow stirring, after which it was cooled to room temperature, dissolved in dichloromethane, and precipitated into either methanol or ethanol. The white solid precipitate was collected by vacuum filtration and dried at 80 °C in vacuo overnight. Yields were typically 94−100%.

Triptycene-Containing Polyester. 1,4-Bis(trimethylsiloxy)benzene (5.016 g, 11.646 mmol, 1 equiv), 1,10-bis(trimethylsiloxy)-decane (11.133 g, 34.940 mmol, 3 equiv), terephthaloyl chloride (9.458 g, 46.585 mmol, 4 equiv). 15.49 g of product was recovered after precipitation from MeOH (>99% yield). ^{1}H NMR ($CDCl_3$, δ): 1.34 (m, 36H), 1.78 (m, 12H), 4.38 (m, 9H), 4.12 (m, 3H), 5.51 (m, 2H), 6.95 (m, 1.5H), 7.02 (m, 4H), 7.35 (m, 4H), 8.10 (m, 12H), 8.28 (m, 2H), 8.42 (m, 2H), 8.58 (m, 0.5H).

Non-Triptycene-Containing Polyester. 1,4-Bis(trimethylsiloxy-)benzene (2.572 g, 10.106 mmol, 1 equiv), 1,10-bis(trimethylsiloxy)decane (9.661 g, 30.320 mmol, 4 equiv), terephthaloyl chloride (8.207 g, 40.423 mmol, 4 equiv). 11.36 g of product was recovered after precipitation from EtOH (97% yeild). ^{1}H NMR ($CDCl_3$, δ): 1.34 (m, 36H), 1.78 (m, 12H), 4.35 (m, 12H), 7.32 (m, 3.5H), 8.10 (s, 12H), 8.22 (m, 4H), 8.28 (m, 4H), 8.37 (s, 0.5H).

Modeling. Accelrys Materials Studio modeling software was used to construct the triptycene models. Discover dynamics smart minimizer with medium convergence for 5000 steps was used to determine the most energetically stable conformation of the structure. The software was also used to calculate the volume occupied by the triptycene units using a van der Waals isosurface.

Thermal Properties and Density. Samples were scanned at 10 °C/min with TA Instruments Q1000 differential scanning calorimeter to obtain values for melting temperature, enthalpy of melting, crystallization temperature, and enthalpy of crystallization from the second heating and cooling cycles according to ASTM D3418-03. The glass transition temperatures were not readily evident from the DSC, so that information was obtained from the tan delta curves.

Thermal gravimetric analysis was used to determine degradation temperatures in air at 5 °C/min with Q50 TGA from TA Instruments. The values for the temperatures at which the highest amount of degradation occurs were obtained from the first derivative of the sample weight vs temperature curve. These were reported as the T_d.

Density measurements were taken using a Micromeritics AccuPyc 1330 He pycnometer by researchers at DuPont.

Mechanical Properties. Films were solvent cast for mechanical testing. Samples were first dissolved in dichloromethane at 60 °C at concentrations of roughly 9 mg/mL. Solutions were then transferred through Target 0.2 μm Teflon filters into custom-machined, rectangular Teflon dishes. Solutions were allowed to evaporate slowly for 48 h at room temperature with a glass cover. To ensure the elimination of all solvent, the films were placed in a vacuum oven at 65 °C for 5 h and then stored in a desiccator under vacuum for 2 days. TGA was used to confirm that the samples were dry of solvent. This procedure produced films of 70−100 μm in thickness. These films were cut with razor blades to produce strips of roughly 50 mm in length and 5 mm in width. The samples were stored in a desiccator to ensure the same level of low water content from sample to sample. Films were also tension heat treated (THT) in the Zwick temperature chamber. Triptycene polyester film samples were heated to 70 °C, strained 400%, and then held in tension as the chamber was allowed to air cool back to room temperature. The films were then removed, measured, and tested for mechanical properties. This procedure resulted in oriented films of roughly 40 μm in thickness. These films were cut with razor blades to produce strips roughly 50 mm in length and 4 mm in width. The non-triptycene polyester samples could not be strained past 20% even at 70 °C. As such small strains would be unlikely to impart significant microstructural changes, non-triptycene polyester films were not tension heat treated for mechanical testing.

A TA Instruments Q1000 dynamic mechanical analyzer was used to acquire storage modulus, loss modulus, and tan delta for films in tension. Films were cyclically strained at 0.15% engineering strain at frequencies of 1 and 10 Hz using a temperature ramp rate of 2 °C/min. The triptycene polyester data were averaged over four samples, while the non-triptycene polyester data was averaged over three samples.

A Zwick/Roell Z010 with a 500 N load cell and PN8133 grips was used to determine the tensile mechanical properties of the prepared films. Using a gauge length of 40 mm and a preload of 1 N, films were strained to failure at a rate of 40 mm/min. The Zwick software was used to determine the Young's modulus, strength, and strain to failure of the films. Mechanical properties data are presented in two categories: average properties and highest individual result. Three samples of the triptycene polyester films exhibited higher stiffnesses (almost 3 standard deviations away) than the rest of the samples. It is likely that these samples contained considerably fewer flaws or defects than the others. Therefore, these three were categorized separately, and the best was reported here under "highest individual result". In the stress−strain plot (Figure 4), these samples were excluded to prevent clutter. The non-triptycene polyester highest individual result data is included in Figure 4 as it did not differ greatly from the average. Data from samples that tore, slipped, or failed outside of the gauge length or at an obvious flaw were discarded in accordance with ASTM D882.

Wide-Angle X-ray Scattering. WAXS patterns were taken using a Molecular Metrology small-angle X-ray scattering system in a modified configuration with a custom-machined attachment such that WAXS *d*-spacings could be observed. All images were normalized for sample thickness, exposure time, and beam flux. The *d*-spacings were calibrated with Al_2O_3 using Polar Software and Fit2D.

Acknowledgment. This work was supported by the U.S. Army through the Institute for Soldier Nanotechnologies under Contract DAAD-19-02-0002 with the U.S. Army Research Office. We thank Dr. Wayne E. Marsh, Dr. Gregory T. Dee,

and Lloyd Abrams from DuPont. We also thank Dr. Tim D. Fornes, Dr. Jeff W. Baur, Dr. Brian D. Pate, Dr. Chaitanya K. Ullal, Numan Waheed, Joseph J. Walish, and Harry Benjamin Larman for their contributions during the course of this work.

References and Notes

(1) Baughman, R. H.; Zakhidov, A. A.; de Heer, W. A. *Science* **2002**, *297*, 787.
(2) Ajayan, P. M.; Stephan, O.; Colliex, C.; Trauth, D. *Science* **1994**, *265*, 1212.
(3) Kumar, S.; Dang, T. D.; Arnold, F. E.; Bhattacharyya, A.; Min, B. G.; Zhang, X.; Vaia, R. A.; Park, C.; Adams, W. W.; Hauge, R. H.; Smalley, R. E.; Ramesh, S.; Willis, P. A. *Macromolecules* **2002**, *35*, 9039.
(4) Usuki, A.; Kojima, Y.; Kawasumi, M.; Okada, A.; Fukushima, Y.; Kurauchi, T.; Kamigaito, O. *J. Mater. Res.* **1993**, *8*, 1179.
(5) Kojima, Y.; Usuki, A.; Kawasumi, M.; Okada, A.; Fukushima, Y.; Kurauchi, T.; Kamigaito, O. *J. Mater. Res.* **1993**, *8*, 1185.
(6) Liaw, D.-J.; Liaw, B.-Y.; Yang, C.-M. *Macromolecules* **1999**, *32*, 7248.
(7) Liaw, D.-J.; Liaw, B.-Y.; Chen, J.-R.; Yang, C.-M. *Macromolecules* **1999**, *32*, 6860.
(8) Dotrong, M.; Dotrong, M. H.; Song, H. H.; Santhosh, U. U.; Lee, C. Y.-C.; Evers, R. C. *Polymer* **1998**, *39*, 5799.
(9) Liaw, D.-J.; Hsu, P.-N.; Chen, W.-H.; Lin, S.-L. *Macromolecules* **2002**, *35*, 4669.
(10) Park, K. H.; Tani, T.; Kakimoto, M.-A.; Imai, Y. *J. Polym. Sci., Part A: Polym. Chem.* **1998**, *36*, 1767.
(11) Oishi, Y.; Ishida, M.; Kakimoto, M.-A.; Imai, Y.; Kurosaki, T. *J. Polym. Sci., Part A: Polym. Chem.* **1992**, *30*, 1027.
(12) van Reenen, A. J.; Mathias, L. J.; Coetzee, L. *Polymer* **2004**, *45*, 799.
(13) Chern, Y.-T.; Shiue, H.-C.; Kao, S. C. *J. Polym. Sci., Part A: Polym. Chem.* **1998**, *36*, 785.
(14) Chern, Y.-T.; Wang, W.-L. *Macromolecules* **1995**, *28*, 5554.
(15) Hsiao, S.-H.; Li, C.-T. *J. Polym. Sci., Part A: Polym. Chem.* **1999**, *37*, 1435.
(16) Espeso, J. F.; de la Campa, J. G.; Lozano, A. E.; de Abajo, J. *J. Polym. Sci., Part A: Polym. Chem.* **2000**, *38*, 1014.
(17) Jeong, H. Y.; Lee, Y. K.; Talaie, A.; Kim, K. M.; Kwon, Y. D.; Jang, Y. R.; Yoo, K. H.; Choo, D. J.; Jang, J. *Thin Solid Films* **2002**, *417*, 171.
(18) Romo-Uribe, A.; Mather, P. T.; Haddad, T. S.; Lichtenhan, J. D. *J. Polym. Sci., Part B: Polym. Phys.* **1998**, *36*, 1857.
(19) Kopesky, E. T.; Haddad, T. S.; Cohen, R. E.; McKinley, G. H. *Macromolecules* **2004**, *37*, 8992.
(20) Zhang, W.; Fu, B. X.; Seo, Y.; Schrag, E.; Hsiao, B.; Mather, P. T.; Yang, N.-L.; Xu, D.; Ade, H.; Rafailovich, M.; Sokolov, J. *Macromolecules* **2002**, *35*, 8029.
(21) Fu, B. X.; Zhang, W.; Hsiao, B. S.; Rafailovich, M.; Sokolov, J.; Johansson, G.; Sauer, B. B.; Phillips, S.; Balnski, R. *High Perform. Polym.* **2000**, *12*, 565.
(22) Long, T. M.; Swager, T. M. *Adv. Mater.* **2001**, *13*, 601.
(23) Kelly, T. R.; Sestelo, J. P.; Tellitu, I. *J. Org. Chem.* **1998**, *63*, 3655.
(24) Iwamura, H.; Mislow, K. *Acc. Chem. Res.* **1988**, *21*, 175.
(25) Hoffmeister, E.; Kropp, J. E.; McDowell, T. L.; Michel, R. H.; Rippie, W. L. *J. Polym. Sci., Part A-1* **1969**, *7*, 55.
(26) (a) Long, T. M.; Swager, T. M. *J. Am. Chem. Soc.* **2002**, *124*, 3826. (b) Zhu, Z.; Swager, T. M. *J. Am. Chem. Soc.* **2002**, *124*, 9670.
(27) Paraskos, A. J. Ph.D. Thesis, MIT, 2003.
(28) Bartlett, P. D.; Ryan, M. J.; Cohen, S. G. *J. Am. Chem. Soc.* **1942**, *64*, 2649.

MA060047Q